

# Pinning modes and interlayer correlation in high magnetic field bilayer Wigner solids

Zhihai Wang,<sup>1,2</sup> Yong P. Chen,<sup>1,3,\*</sup> L. W. Engel,<sup>1</sup> D. C. Tsui,<sup>3</sup> E. Tutuc,<sup>2,†</sup> and M. Shayegan<sup>3</sup>

<sup>1</sup>*National High Magnetic Field Laboratory, 1800 E. Paul Dirac Drive, Tallahassee, FL 32310*

<sup>2</sup>*Department of Physics, Princeton University, Princeton, NJ 08544*

<sup>3</sup>*Department of Electrical Engineering, Princeton University, Princeton, NJ 08544*

(Dated: March 23, 2022)

We report studies of pinning mode resonances in the low total Landau filling ( $\nu$ ) Wigner solid of a series of bilayer hole samples with negligible interlayer tunneling, and with varying interlayer separation  $d$ . Comparison of states with equal layer densities ( $p, p$ ) to single layer states ( $p, 0$ ) produced *in situ* by biasing, indicates that there is interlayer quantum correlation in the solid at small  $d$ . Also, the resonance frequency at small  $d$  is decreased just near  $\nu = 1/2$  and  $2/3$ , indicating the importance in the solid of correlations related to those in the fractional quantum Hall effects.

Bilayers, closely spaced sheets of carriers in semiconductor hosts, exhibit phenomena that arise from interlayer interaction and quantum correlation and so are not present in single layers. Of particular importance is the quantum Hall (QH) state at total bilayer Landau filling factor  $\nu = 1$ , for the case of small interlayer separation and weak interlayer tunneling. Owing to striking phenomena, both in magnetotransport [1, 2] and in interlayer tunneling [3], that state is understood to have carrier wave functions which extend coherently between the two layers, with the difference in the quantum phase between the layers spontaneously developing long range spatial coherence over the plane. This  $\nu = 1$  state can be thought of as bilayer exciton condensate, excitonic counterflow superfluid, or a pseudospin ferromagnet with magnetization in the plane. As usual in describing bilayer states, pseudospin specifies the layer.

Interlayer quantum correlation, in the sense of wave functions spreading coherently between layers when tunneling is small, is present in bilayers at other  $\nu$  than one. Such interlayer correlation underlies the  $\nu = 1/2$  [4, 5, 6] and  $3/2$  [6, 7] fractional QH effects (FQHE) observed in bilayers. This work will focus on interlayer correlation within bilayer Wigner crystal (BWC) phases [8, 9, 10], in samples with negligible interlayer tunneling. Wigner crystals, lattices stabilized by repulsion between carriers, have been predicted in the absence of disorder [11, 12] for bilayers, as well as for single layer systems [13], at the low  $\nu$  termination of the QH series.

Theories [11, 12, 14] have predicted a number of distinct BWC phases. The relative importance of interlayer and intralayer interaction is crucial in these theories, and is measured by the ratio  $d/a$ , where  $d$  is the center-to-center layer separation,  $a = (2\pi p)^{-1/2}$  is the mean in-plane carrier spacing and  $p$  is the carrier density per layer. A one component triangular lattice is expected at small enough  $d/a$ , and is an easy plane pseudospin ferromagnetic BWC (FMBWC) with one carrier, evenly and coherently spread between the two layers, at each lattice site. Interlayer-staggered two component lattices occur at larger  $d/a$ , and without interlayer tunneling, are pseudospin antiferromagnetic BWCs (AFMBWC), with car-

riers essentially completely in one layer alternating with those completely in the other. Multiple staggered two component phases are predicted, including square and rectangular lattices. For  $d \gg a$ , the intralayer interaction dominates, so the layers are simply triangular lattices like single layer Wigner crystals, but interlayer-staggered.

Wigner crystals in real samples, bilayer or single layer, are pinned by disorder, and so are insulators. Pinning also produces a striking microwave or rf conductivity resonance, or “pinning mode”, which is a collective oscillation of the carriers about their pinned positions. Pinning mode resonances of single layers have been studied experimentally [15, 16, 17, 18, 19, 20] and theoretically [21, 22, 23] and have proven to be valuable for obtaining information about single layer, pinned Wigner solids. The resonance frequency always increases as the disorder strength increases, and is also sensitive [21, 22, 23] to the correlation length of the effective disorder, which takes into account the spread of the carrier wave functions. Pinning modes of bilayers [24] have also been observed.

We present a systematic study of the pinning mode in a series of bilayer samples, which have negligible interlayer tunneling and widely varying layer separations. For comparison with work on the  $\nu = 1$  excitonic condensate [1, 2, 3], we present the effective layer separation as  $\tilde{d} = d/l_B = 2^{1/2}d/a$ , where  $l_B$  is the magnetic length at  $\nu = 1$  in the balanced state. To isolate effects of interlayer interaction or quantum correlation, we compare spectra of balanced states (layer carrier densities ( $p, p$ )) to those of single layers (layer densities ( $p, 0$ )) created *in situ* by depleting one of the layers. Denoting the resonance frequencies in these states by  $f_{pp}$  and  $f_{p0}$ , we focus on  $\eta = f_{pp}/f_{p0}$  vs  $\tilde{d}$ , which has a distinct minimum at  $\tilde{d} \approx 1.8$ . The interpretation is in terms of two competing effects, which respectively tend to lower and raise  $\eta$  as  $\tilde{d}$  decreases: 1) turn-on of the interlayer interaction on going from the ( $p, 0$ ) single layer to the ( $p, p$ ) BWC and 2) enhancement [25] of the effective pinning disorder in the ( $p, p$ ) state relative to that in the ( $p, 0$ ) state *only when the ( $p, p$ ) state is an interlayer quantum correlated FMBWC*. Of importance as well, and present only for

small  $\tilde{d}$ , are distinct dips in  $f_{pp}$  vs  $B$ , around  $\nu = 1/2$  or  $2/3$ , demonstrating the effect, within the low  $\nu$  BWC insulator, of correlations present in the FQHE states.

The samples, described in Table I, are GaAs double quantum well hole systems grown on (311)A substrates. Each wafer has a pair of 150 Å GaAs wells, which are separated by AlAs barriers for  $d \leq 300$  Å, and a combination of AlAs and AlGaAs for  $d > 300$  Å. All the wafers are designed to have negligible interlayer tunneling.  $\text{Re}(\sigma_{xx})$  vs  $B$  traces, like those in Fig. 1b, show a dip around  $\nu = 1$  for the lower  $\tilde{d}$  samples. The absence of this dip for  $\tilde{d} \geq 1.69$  nearly agrees with earlier results [1, 3], in which the  $\nu = 1$  state is present for  $\tilde{d} \leq 1.8$ .

We performed microwave measurements using a method that has been described earlier [18, 19, 20]. A coplanar waveguide (CPW) transmission line, on top of the sample, couples capacitively to the bilayer, as shown schematically in Fig. 1a. The CPW has a narrow, driven center conductor separated from grounded side planes by slots of width  $W$ . The measurements proceed in a high frequency, low loss limit of the CPW, in which the microwave field is only slightly perturbed by the conductivity of the bilayer. In this case the in-plane microwave electric field 1) is mainly confined to the region immediately under the slots, and 2) is essentially the same in both layers. We calculated the real part of diagonal conductivity from the transmitted power  $P$  using a formula valid in this limit, when reflections are minimal,  $\text{Re}(\sigma_{xx}) = -W |\ln(P/P_0)| / 2Z_0 L$ , where  $P_0$  is the transmitted power with all carriers depleted from the bilayer,  $Z_0 = 50 \Omega$  is the characteristic impedance calculated for the CPW geometry with  $\sigma_{xx} = 0$ , and  $L$  is the length of the CPW. The data, all taken around 60 mK, were obtained in the low power limit, in which further power reduction did not affect the measured  $\text{Re}(\sigma_{xx})$ . A voltage applied between a backgate and contacts to both layers

Wafer	$d$ (Å)	$p$ ( $10^{10} \text{ cm}^{-2}$ )	$\tilde{d}$	$\nu = 1$ QHE
M440	225	3.00	1.38	yes
M465	230	3.65	1.56	yes
M417	260	2.70	1.51	yes
		3.05	1.61	yes
M433	300	2.52	1.69	no
		2.85	1.80	no
M436	450	2.40	2.47	no
M443	650	2.85	3.89	no
M453	2170	5.3	18	no

TABLE I: Sample parameters in balanced states: center-to-center well separation ( $d$ ), density per layer ( $p$ ) and effective separation  $\tilde{d} = d/l_B$ , where  $l_B = (4\pi p)^{-1/2}$  is the magnetic length at total filling factor  $\nu = 1$ . The two  $p, \tilde{d}$  for M417 and M433 are from different cooldowns. The last column states if a minimum in  $\text{Re}(\sigma_{xx})$  vs magnetic field at  $\nu = 1$  is present.

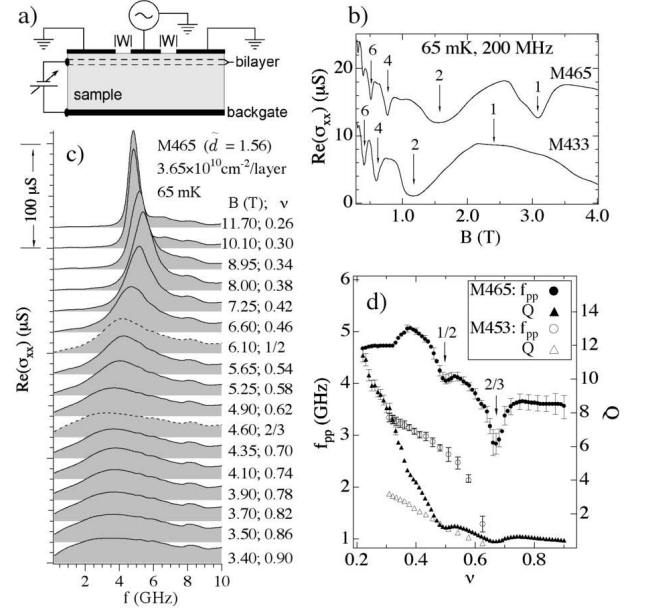


FIG. 1: a) Magnified cross section, not to scale, through the transmission line and sample. b) Real part of diagonal conductivity  $\text{Re}(\sigma_{xx})$  vs. magnetic field,  $B$ , for M465, and M433, in their balanced states. Total Landau filling factors,  $\nu$ , are marked. c)  $\text{Re}(\sigma_{xx})$  vs frequency,  $f$ , for M465 in its balanced state, for many  $B$ , (or  $\nu$ ). Spectra are vertically displaced proportional to  $\nu$  and shaded downward to their zeros. d) peak frequency  $f_{pp}$  and  $Q$  vs  $\nu$  ( $Q$  is  $f_{pp}$  divided by full width at half maximum).

was used to control the layer densities.

The microwave measuring method precludes the use of front (top) gates to allow independent tuning of the top and bottom layer densities. A metal film too close to the slots would effectively shield the bilayer from the required in-plane microwave field. Hence, a balanced state is produced only by tuning the backgate voltage and can for each cooldown be produced at only one density. For comparison with balanced bilayer states with layer densities  $(p, p)$ , we realize a single layer state  $(p, 0)$  *in situ*, by reducing the total density, as evaluated from QH features, by 50% from that in the balanced state.

Figure 1b shows  $\text{Re}(\sigma_{xx})$  vs  $B$  for M465 and M433, in their balanced states, measured at  $f = 200$  MHz. It shows that the main features observed [2, 9, 26] in dc transport are still readily observable with the transmission line. M465, with  $\tilde{d} \approx 1.56$  exhibits the  $\nu = 1$  IQHE, while M433, with  $\tilde{d} \approx 1.8$ , does not. We used rf traces like these to assess the total density and also to find the balanced states, by adjusting the backgate voltage, to minimize the strength of the  $\nu = 1$  feature (for M440, M465, and M417) [9], or to minimize the hysteresis in  $B$  of QH states (for M433, M436, M443, and M453) [26].

Figure 1c illustrates the evolution with  $B$  (and  $\nu$ ) of the spectra of M465 in its balanced state. Parameters from the spectra,  $f_{pp}$  and  $Q$  ( $f_{pp}$  divided by full width at

half maximum linewidth), are plotted vs  $\nu$  in Fig. 1d. In M465, and the other two samples (M417 and M440) with the smallest  $\tilde{d}$ , the resonance is present for  $\nu$  just below the  $\nu = 1$  QH minimum, and sharpens dramatically as  $\nu$  decreases below about 0.5, so that the  $Q$  vs  $\nu$  curve in Fig. 1d shows a change of slope at that filling.

In the samples with  $\tilde{d} \geq 1.69$ , the resonance appears as  $\nu$  decreases below about 0.6, with gradually increasing  $f_{pp}$  and  $Q$ . This resonance development is typical of that seen at the same per-layer filling, previously [19] in low density p type single layers, and in the present samples in their single layer  $(p, 0)$  states.  $f_{pp}$  and  $Q$  for M453, which has the largest  $\tilde{d}$ , and therefore essentially independent layers, are plotted vs  $\nu$  in Fig. 1d as well.

M465 shows clear dips in  $f_{pp}$  vs  $\nu$  around  $\nu = 1/2$  and  $2/3$  in the plot in Fig. 1c. (M417 and M440 have weak dips in  $f_{pp}$  at  $2/3$  or  $1/2$ , but the dips in those samples are not nearly as clear as in M465, possibly due to the higher  $p$  of M465.) The resonance is well-developed at these fillings, which are well within the insulating phase of this sample, so we do not interpret the dips as FQHE liquid ground states [4, 5, 6, 7], but rather as evidence that some of the correlations related to the FQHE are present in the pinned BWC. In general, as we discuss in more detail below, as Wigner solid moduli increase, the resonance frequency decreases [20, 21, 22, 23]; hence the dips in  $f_{pp}$  correspond either to *increases* in BWC stiffness, or to decreases in the effective carrier-disorder interaction. A decrease in resonance frequency as  $\nu$  approaches an FQHE has been observed [17] in single layer samples. The  $1/2$  FQHE has no analog in the single layer case, and is interlayer correlated, though the  $2/3$  feature can be explained with intralayer correlation. Composite fermion theories [27, 28] have predicted that correlations related to the FQHE are important in single layer, low  $\nu$  Wigner solids.

The main results of this paper follow from direct comparison, for each sample, of the balanced  $(p, p)$  and single layer  $(p, 0)$  states. Spectra from these pairs of states are shown for four samples, at  $B = 10$  T in Fig. 2a-d. The bilayer spectra are shown as solid lines, and the single layer spectra are dashed.  $\text{Re}(\sigma_{xx})$  from the single layer states is doubled to facilitate comparison. The M453 spectra in Fig. 2d are nearly identical, as expected for independent layers, and not surprising considering the large  $\tilde{d} \approx 18$  for that sample. Important for the interpretation below, the nearly identical spectra also indicate that the disorder statistics relevant to the pinning mode are essentially the same in the top and bottom wells. The disorders of the two layers should likewise be similar for all the samples, since they all had similar growth characteristics, such as asymmetrical doping and interfacial compositions.

Hence we interpret the differences between the  $(p, p)$  and  $(p, 0)$  spectra in Fig. 2a-d as due to changes in inter-layer interaction and correlation. Relative to the  $(p, 0)$  spectra, the  $(p, p)$  spectra shift slightly to lower frequency

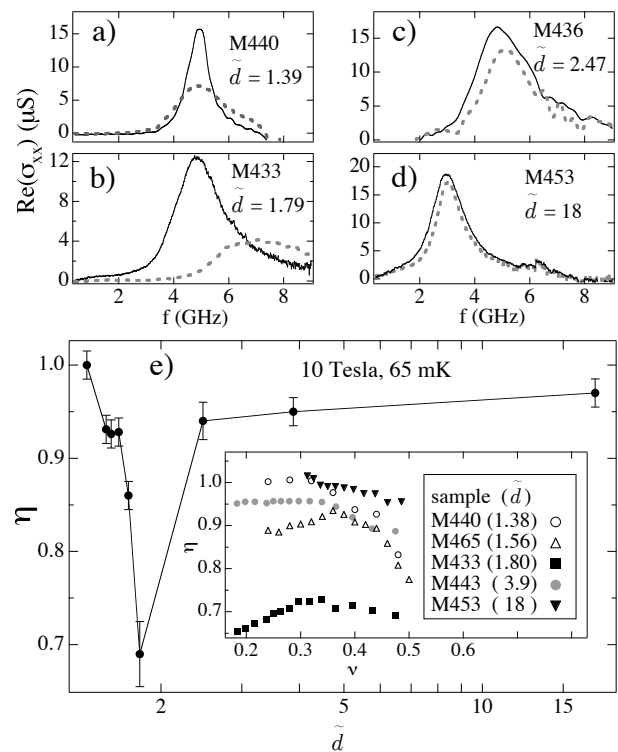


FIG. 2: a)- d) For four samples, the spectrum in the balanced state with layer densities  $(p, p)$  (solid line) is plotted along with the spectrum (with the measured  $\text{Re}(\sigma_{xx})$  multiplied by two) of the single layer state  $(p, 0)$  (dotted line), all at magnetic field  $B = 10$  T. (e)  $\eta = f_{pp}/f_{p0}$  at 10 T vs  $\tilde{d} = d/(4\pi p)^{1/2}$ , where  $f_{pp}$ ,  $f_{p0}$  are the peak frequencies for the  $(p, p)$  and  $(p, 0)$  states and  $d$  is layer separation. Inset:  $\eta$  vs  $\nu$ , the total filling in the bilayer  $(p, p)$  state, for five samples.

as  $\tilde{d}$  decreases down to 2.47, as shown in Fig. 2c. At  $\tilde{d} \approx 1.8$  though, for M433 as shown in Fig. 2b, the  $(p, p)$  spectrum is markedly shifted downward in frequency, and is stronger and sharper. But decreasing  $\tilde{d}$  further (even through a different cooldown of the same M433 sample) reduces the downward shift of  $f_{pp}$  relative to  $f_{p0}$ , though the  $(p, p)$  spectra remain much sharper than the  $(p, 0)$  spectra, as seen in Fig. 2a. To summarize, Fig. 2e shows the ratio  $\eta = f_{pp}/f_{p0}$  vs  $\tilde{d}$ ; this curve has a striking minimum at  $\tilde{d} \approx 1.8$ . Inset in Fig. 2e is a graph of  $\eta$  vs  $\nu$ , the total filling of the  $(p, p)$  states, for several samples. This graph shows that the minimum in  $\eta$  vs  $\tilde{d}$  remains, whether  $B$  or  $\nu$  is fixed, as long as  $\nu \lesssim 0.5$ . For  $\tilde{d} \leq 1.8$ , as shown for M465 in Fig. 1b and c, resonances become markedly sharper below  $\nu \approx 0.5$ .

We interpret the  $\eta$  vs  $\tilde{d}$  curve as a result of two competing effects. The first effect is driven by carrier-carrier interaction and must be present in any weakly pinned Wigner crystal, bilayer or single layer. In this effect, when carrier-carrier interaction is increased, by decreasing their spacing (or increasing their overall density), the resonance frequency decreases. In single layers at fixed

$B$ , at which the resonance is well developed, as carrier density  $n_s$  is decreased, the peak frequency  $f_{pk}$  always increases and the resonance broadens. Typically [18, 20],  $f_{pk} \propto n_s^{-\gamma}$ , with  $\gamma \approx 3/2$  for higher  $n_s$  giving way to  $\gamma \approx 1/2$  at lower  $n_s$ ; the present samples in single layer states all have  $\gamma \approx 1/2 \pm 10\%$ . The interpretation in weak pinning [20, 21, 22, 23] of the increase of  $f_{pk}$  with decreasing  $n_s$  is that reduction of carrier-carrier interaction (*i.e.*, the crystal stiffness) causes the carriers to adjust to positions which essentially fall more deeply into the impurity potential. This increases the pinning energy per carrier, and the restoring force on the carriers, hence  $f_{pk}$ .

We interpret the decrease of  $\eta$  with decreasing  $\tilde{d}$ , for  $\tilde{d} \geq 1.8$ , as due to this carrier-carrier interaction effect, within an AFMBWC. The result of this effect, on going from  $(p, 0)$  to  $(p, p)$  in the limit of small  $\tilde{d}$ , is analogous to doubling the areal density of a single layer, and for  $\gamma \sim 1/2$  gives  $\eta = 2^{-\gamma} \approx 0.71$ . This agrees with the  $\eta$  we measure for  $\tilde{d} \approx 1.8$ . The sharp increase in  $\eta$  as  $\tilde{d}$  goes below 1.8 is not readily explainable in terms of the carrier-carrier interaction effect. Transitions between different types of AFMBWC are predicted by the theories [11, 12, 14] and if  $\tilde{d}$  is near a transition, the BWC can conceivably soften (multiple low energy arrangements become possible), producing some increase of  $\eta$  around particular  $\tilde{d}$ . It is not likely though, that even around a transition between AFMBWC phases,  $\eta$  would be as close to unity as it is in Fig. 2e at the smallest  $\tilde{d}$  values.

The second competing effect that we use to explain  $\eta$  vs  $\tilde{d}$  is driven by interlayer correlation, is present only in the FMBWC, and was considered theoretically by Chen [25]. Chen found that in an FMBWC pinning is enhanced when there is disorder that is spatially correlated in the planes of the top and bottom layers. At sites where impurities or interfacial features induce local interlayer tunneling [2], such spatial correlation would naturally result. When this disorder enhancement is considered [25] along with the competing carrier-carrier interaction effect,  $\eta$  as large as  $2^{1-\gamma}$  is possible, so the transition to an FMBWC is sufficient to explain the increase of  $\eta$  with decreasing  $\tilde{d}$  seen in Fig. 2e for  $\tilde{d} \lesssim 1.8$ . Even within the FMBWC, an increase of  $\eta$  as  $\tilde{d}$  decreases is expected, since the smaller  $\tilde{d}$  would increase the interlayer-spatially correlated component of effective disorder.

The data then indicate that  $\tilde{d}^*$ , the critical  $\tilde{d}$  below which the FMBWC is present, is around 1.8. Theories with small but finite tunneling predict smaller  $\tilde{d}^*$ , around 0.4 [11, 12]. A possible explanation of the discrepancy lies in the increased pinning experienced by the FMBWC, since the pinning energy can stabilize the FMBWC against the more weakly pinned AFMBWC phases that succeed it at larger  $\tilde{d}$ . It is likely that pinning energy plays a role in stabilizing single layer Wigner crystals against the FQHE liquid at high fillings [29], and against melting at elevated temperatures [16]. A possi-

ble clue to the presently estimated  $\tilde{d}^* \approx 1.8$  is that it is close to the maximal  $\tilde{d}$  values below which the interlayer correlated QH states at  $\nu = 1$  and  $1/2$  exist, respectively  $\tilde{d} \approx 1.8$  [1, 3] and 2 [4].

In sum, our systematic studies of pinning modes of BWC have found effects of interlayer interaction and give evidence for BWC interlayer correlations in which the wave function of a carrier spreads evenly between the two layers. Correlations related as precursors to the bilayer  $1/2$  and  $2/3$  FQHEs are also present in the BWC.

We thank N. Bonesteel, H. A. Fertig and Kun Yang for discussions, and acknowledge the support of AFOSR and DOE. NHMFL is supported by NSF grant DMR-0084173, the State of Florida, and DOE.

---

\* Current address: Rice University, Houston, TX

† Current address: University of Texas, Austin, TX

- [1] M. Kellogg *et al.*, Phys. Rev. Lett. **93**, 036801 (2004).
- [2] E. Tutuc, M. Shayegan, and D. A. Huse, Phys. Rev. Lett. **93**, 036802 (2004).
- [3] I. B. Spielman *et al.*, Phys. Rev. Lett. **84**, 5808 (2000); *ibid.*, **87**, 036803 (2001).
- [4] J. P. Eisenstein *et al.*, Phys. Rev. Lett. **68**, 1383 (1992).
- [5] Y. W. Suen *et al.*, Phys. Rev. Lett. **68**, 1379 (1992).
- [6] Y. W. Suen *et al.*, Phys. Rev. Lett. **72**, 3405 (1994).
- [7] A. R. Hamilton *et al.*, Phys. Rev. B **54**, 5259 (1996).
- [8] H. C. Manoharan *et al.*, Phys. Rev. Lett. **77**, 1813 (1996).
- [9] E. Tutuc *et al.*, Phys. Rev. Lett. **91**, 076802 (2003).
- [10] S. Faniel, *et al.*, Phys. Rev. Lett. **94**, 046802 (2005).
- [11] S. Narasimhan and T. L. Ho, Phys. Rev. B **52**, 12291 (1995).
- [12] L. Zheng and H. A. Fertig, Phys. Rev. B **52**, 12282 (1995).
- [13] Y. E. Lozovik and V. I. Yudson, JETP Lett., **22**, 11 (1975); P. K. Lam and S. M. Girvin, Phys. Rev. B **30**, 473 (1984); D. Levesque, J. J. Weis and A. H. McDonald, Phys. Rev. B **30**, 1056 (1984); Kun Yang, F. D. M. Haldane, and E. H. Rezayi Phys. Rev. B **64**, 081301 (2001).
- [14] G. Goldoni and F. M. Peeters, Phys. Rev. B **53**, 4591 (1996).
- [15] See G. Sambandamurthy, *et al.*, Solid State Comm. **140**, 100 (2006) for a brief review.
- [16] Yong P. Chen, *et al.*, Nature Physics **2**, 452 (2006).
- [17] Yong P. Chen, *et al.*, Phys. Rev. Lett. **93**, 206805 (2004).
- [18] P. D. Ye *et al.*, Phys. Rev. Lett. **89**, 176802 (2002).
- [19] C.-C. Li *et al.*, Phys. Rev. Lett. **79**, 1353 (1997);
- [20] C.-C. Li *et al.*, Phys. Rev. B **61**, 10905 (2000).
- [21] R. Chitra, T. Giamarchi, P. Le Doussal, Phys. Rev. Lett. **80**, 3827 (1998); *ibid.* Phys. Rev. B **65**, 035312 (2002).
- [22] H. A. Fertig, Phys. Rev. B **59**, 2120 (1999).
- [23] M. M. Fogler and D. A. Huse, Phys. Rev. B **62**, 7553 (1999).
- [24] J. B. Doveston *et al.*, Physica E **12**, 296 (2002).
- [25] Yong P. Chen, Phys. Rev. B **73**, 115314 (2006).
- [26] E. Tutuc *et al.*, Phys. Rev. B **68**, 201308 (2003).
- [27] R. Narevich, G. Murthy and H. A. Fertig, Phys. Rev. B **64**, 245326 (2001).
- [28] C.-C. Chang, G. S. Jeon, and J. K. Jain, Phys. Rev. Lett.

**94**, 016809 (2005).

[29] R. Price *et al.*, Phys. Rev. B **48**, 11473, (1993).